

Investigating the Vision Transformer Model for Image Retrieval Tasks

Socratis Gkelios
Department of Electrical and
Computer Engineering
Democritus University of Thrace
Xanthi, Greece.
sgkelios@ee.duth.gr

Yiannis Boutalis
Department of Electrical and
Computer Engineering
Democritus University of Thrace
Xanthi, Greece.
ybout@ee.duth.gr

Savvas A. Chatzichristofis
Intelligent Systems Laboratory
Department of Computer Science
Neapolis University Pafos
Pafos, Cyprus
s.chatzichristofis@nup.ac.cy

Abstract—This paper introduces a plug-and-play descriptor that can be effectively adopted for image retrieval tasks without prior initialization or preparation. The description method utilizes the recently proposed Vision Transformer network while it does not require any training data to adjust parameters. In image retrieval tasks, the use of Handcrafted global and local descriptors has been very successfully replaced, over the last years, by the Convolutional Neural Networks (CNN)-based methods. However, the experimental evaluation conducted in this paper on several benchmarking datasets against 36 state-of-the-art descriptors from the literature demonstrates that a neural network that contains no convolutional layer, such as Vision Transformer, can shape a global descriptor and achieve competitive results. As fine-tuning is not required, the presented methodology's low complexity encourages adoption of the architecture as an image retrieval baseline model, replacing the traditional and well adopted CNN-based approaches and inaugurating a new era in image retrieval approaches.

Index Terms—Vision Transformer, Image Retrieval, CBIR

I. INTRODUCTION

Content-based image retrieval (CBIR) is one of the fundamental scientific challenges that the multimedia, computer vision, and robotics communities have thoroughly researched for decades. Three eras that vary in how researchers export the different features that define an image's visual content characterize content-based image retrieval [1]. The literature strongly focuses on global low-level descriptors during the early years, shaping the first CBIR era. A single vector was used to represent different aspects of an image, such as color, shape, and texture. In the sequel, the community started to concentrate on representations focused on the extraction and use of local features. From 2003 onwards, new approaches adopt local image descriptors to search for salient image patches and points-of-interest, such as edges, corners, and blobs. Since 2015, image retrieval research strongly relies on approaches focused on Deep Learning (DL) and Convolutional Neural Networks (CNN). Although DL-based techniques require a large amount of data for training, the pre-trained networks have been demonstrated in several studies to be particularly useful as feature extractors and achieve high retrieval performance.

Meanwhile, in natural language processing (NLP), the self-attention-based architecture, particularly *Transformers*, is now considered as the new standard [2]. The Transformer is a type of deep-neural network mainly based on self-attention mechanism [3]. Recently, researchers have expanded transformers for computer vision tasks inspired by the influence of the Transformer in NLP [4]–[6]. For example, the authors in [7] have trained a sequence transformer to auto-regressively predict pixels and achieve competitive results with CNNs on an image classification task. Recently, the authors in [8] have attempted to apply a typical transformer directly to images, with the fewest adjustments possible shaping an image recognition network. Vision Transformer network (ViT) provides better performance than a traditional convolutional neural network in image recognition tasks.

This paper builds upon the Vision Transformer architecture to shape a global descriptor for image retrieval tasks. Following the procedure that the vast majority of the deep-learning-based image retrieval models adopt, we discard the fully connected layers of the Transformer's network and use the last layer as a feature to describe the visual content of the image. Best we can tell, this is the first attempt to evaluating the performance of the transformers on image retrieval tasks.

The remainder of this paper is structured as follows. Section II briefly shows how the vision transformer's architecture operates and presents the process of shaping the image retrieval descriptor. Section III offers a thorough experimental evaluation of the descriptor complemented by a discussion of results. Finally, Section IV concludes the paper, and discusses potential opportunities for future work.

II. ViT DESCRIPTOR

The Transformer architecture was first introduced in [2] for neural machine translation exhibiting state-of-the-art performance and replacing models, such as Long short-term memory artificial recurrent neural networks and Gated recurrent units (GRUs) in several Natural Language Processing (NLP) tasks. The architecture of the Transformer usually consists of stacked Transformer layers, each of which takes as input a sequence of vectors and outputs a new sequence of vectors of the same shape. The critical element of the Transformer architectures

*Corresponding author: s.chatzichristofis@nup.ac.cy

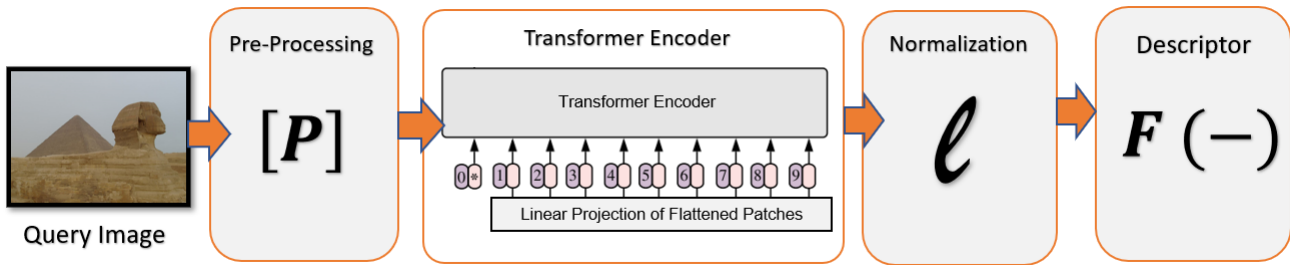


Fig. 1. Graphical Abstract of the ViT Extraction Procedure.

resides in the attention mechanism. The transformer development’s primary motivation was to overcome the limitations of the recurrent neural networks (RNN) and mainly to capture long-term global dependencies. Based on this foundation, many noteworthy approaches emerged, for example, Bidirectional Encoder Representations from Transformers (BERT) [9], and GPT-3 [10], both pre-trained in an unsupervised manner from the unlabeled text. These methods demonstrated rich representation capability without fine-tuning. Both methods are conceptually simple and empirically powerful.

The application of Transformers in computer vision tasks poses a significant challenge for two main reasons:

- Images contain much more information compared to words or sentences.
- Attention to every pixel is computationally exhaustive.

The authors in [8] proposed a novel approach called Vision Transformer (ViT) to tackle these challenges. ViT borrows the encoder part of the NLP Transformer. The standard Transformer receives a 1D token embedding sequence as input. In this case, the images are split into fixed-sized patches and feed into the model. A learnable positional embedding vector is assigned to every patch to utilize the order of the input sequence. Besides, a special token is added, just like in the case of BERT. In a nutshell, a set of patches is constructed for each image multiplied with an embedding matrix, which is finally fused with a positional embedding vector, forming the Transformer input. In all its layers, the Transformer uses constant latent vector size, so with a trainable linear projection, the patches are flattened to map these dimensions. This projection’s output is referred to as patch embedding.

Each encoder consists of two sub-layers. In the first sub-layer, the inputs flow through a self-attention module, while in the second, the outputs of the self-attention operation are passed to a position-wise feed-forward neural network. Furthermore, skip connections [11] are incorporated around each sub-layer that undergo layer normalization. The architecture of the encoder is depicted in Figure 2. Every layer contains a constant linear projection mapping of the flattened patches of dimension D refined during training. D is equal to 768 for ViT-B architectures, whereas in ViT-L, the corresponding value is 1024. Even though the encoder layers are composed of identical structural elements, they do not share weights.

The self-attention module consists of three learnable components, Query (Q), Key (K), and Value (V). A score matrix is assembled by Q and K dot product multiplication that portrays the attention of each ‘word’ to each other ‘word’ (in our approach, each ‘word’ corresponds to one of the image patches). The score matrix is scaled accordingly and is passed to a softmax layer to convert scores into probabilities. In the sequel, the softmax output is multiplied with the V vector to highlight the important words. Multi-headed attention improves the performance of the Transformer. In particular, the model performs multiple parallel attention functions to different linear projections of the vectors Q, V, and K instead of utilizing a single one. Thus, this procedure enables the model to focus on different positions and representation subspaces.

Position-wise neural network module is a fully connected feed-forward neural network (FFNN), which consists of two linear transformations with a ReLU activation in between. Layer LayerNorm (LN) is applied before each module, and residual connections after every block, followed by layer normalization [12].

In this paper, we adopted the pre-trained architecture of [8]. More specifically, this paper adopts the ‘Base’ models (ViT-B) and the ‘Large’ models (ViT-L) from BERT. Two variants of each architecture regarding their input patch size are applied. ViT-L16 corresponds to 16×16 input batch size, while ViT-L32 to 32×32 patch size. The same notations are used for the ViT-B model accordingly. The models with smaller patch sizes are more resource-intensive due to the inversely proportional relationship between the Transformer’s length sequence and the patch size square.

The adopted architectures have been trained on 21k-ImageNet (21k classes/14 million images) and have been fine-tuned on the ILSVRC-2012 ImageNet (1k classes/1.3 million images) [13]. ViT-B features 12 encoder layers with an FFNN of size 3072. On the other hand, ViT-L contains 24 encoder layers and an FFNN of size 4096.

In the case of ViT descriptor, initially, all the images are resized to 384×384 pixel size. A pre-preprocessing unit subtracts 127.5 to all pixels and scales by 255 to have pixel values ranging $[-1, 1]$. The pre-processed images flow through the Transformer Encoder. The last softmax layer of the models is removed, leaving the normalized last encoder’s output of dimension D as the final layer. This procedure shapes a representation vector for each image. The final step

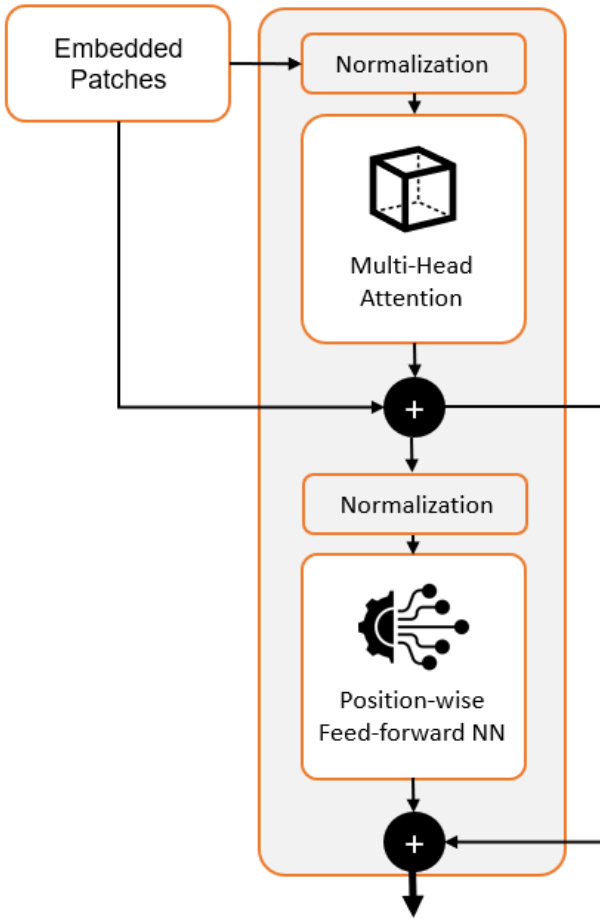


Fig. 2. Modelling the Transformer Encoder Architecture.

is comprised of a normalization procedure to shape the ViT descriptor. Figure 1 illustrates the proposed CBIR architecture.

III. EXPERIMENTAL SETUP

This section provides details about the experiments conducted for the evaluation of the ViT descriptor. The presented image representation is evaluated on four well-known image datasets:

- INRIA Holidays [14]: This dataset consists of 1491 cellphone-taken pictures with a wide range of holiday scenes and objects. The number of images varies from 2 to 13 images per group. The INRIA Holidays dataset provides many query images instead of the UKBench database. The ground truth comprises images of a visual definition identical to the query image, without indicating the same object's co-occurrence.
- UKBench [15]: The UKBench dataset consists of 10,200 images arranged in 2250 categories dataset. There are four pictures of a single object in each category, taken from various views and under varying lighting conditions. The top-4 candidate (NS) score [15] is used for this dataset during the evaluation process to calculate the retrieval accuracy.

- Paris6K [16]: 6412 photographs representing unique Paris landmarks are included in the Paris6k Dataset. This collection consists of 55 pictures of buildings and monuments from requests. There is more variety in the landmarks in Paris6k than those in Oxford5k.
- Oxford5k [17]: This building's dataset is made up of 5062 Flickr images. The set has been manually annotated to produce a detailed ground truth for 11 distinct landmarks, each represented by five potential queries. The index, overall, consists of 55 requests. In this dataset, completely different views of the same building are labeled by the same name, making the collection challenging for image retrieval tasks [18].

For the INRIA, Oxford5k, and Paris6K datasets, the mean Average Precision (mAP) [19] is used as an evaluation metric. In the perfect retrieval case, mAP is equal to 100, while as the number of the nonrelevant images ranked above a retrieved relevant image increases, the mAP approaches the value 0. On the other hand, the retrieval performance on the UKBench dataset is evaluated using the recall rate for the top-4 candidates (NS) as an evaluation metric. In the case of perfect retrieval, NS is equal to 4.

To calculate the similarity between the descriptors, we use multiple distance metrics. There are specific advantages and drawbacks of each similarity metric, each one being more appropriate for particular data types [20]. This paper assesses the use of Manhattan, Euclidean, Cosine, Bray-Curtis, Canberra, Chebyshev, and Correlation distance metrics in the current analysis. The Manhattan and Euclidean distance metrics are considered well-known, and therefore, no further details are given in this paper. Here we only note that the Manhattan Distance (also known as city block distance) is preferred over the Euclidean distance metric as the data's dimension increases.

The Cosine distance counts the image descriptors' inner-product space, considering their orientation and not their magnitude.

$$d_{Cosine}(\mathbf{p}, \mathbf{q}) = \frac{\mathbf{p}\mathbf{q}}{\|\mathbf{p}\|\|\mathbf{q}\|} = \frac{\sum_{i=1}^n p_i q_i}{\sqrt{\sum_{i=1}^n (p_i)^2} \sqrt{\sum_{i=1}^n (q_i)^2}} \quad (1)$$

Bray-Curtis and Canberra are mutated from Manhattan, where, as seen in the following equation, the sum of the differences between the coordinates of the vectors is normalized:

$$d_{Canberra}(\mathbf{p}, \mathbf{q}) = \sum_{i=1}^n \frac{|p_i - q_i|}{|p_i| + |q_i|} \quad (2)$$

$$d_{Bray-Curtis}(\mathbf{p}, \mathbf{q}) = \frac{\sum_{i=1}^n |p_i - q_i|}{\sum_{i=1}^n (p_i + q_i)} \quad (3)$$

Furthermore, the Chebyshev distance between two feature vectors is estimated as the maximum variation along any coordinate dimension:

$$d_{Chebyshev}(\mathbf{p}, \mathbf{q}) = \max_i (|p_i - q_i|) \quad (4)$$

Finally, the Correlation distance measures the dependency between the two feature vectors:

$$d_{Correl.}(\mathbf{p}, \mathbf{q}) = \frac{\sum_{i=1}^n (p_i - \bar{p})(q_i - \bar{q})}{\sqrt{\sum_{i=1}^n (p_i - \bar{p})^2} \sqrt{\sum_{i=1}^n (q_i - \bar{q})^2}} \quad (5)$$

In all metrics, p and q are the corresponding image descriptors.

Additionally, this section also evaluates the appropriate normalization technique. The batch normalization technique promotes training by specifically normalizing each layer’s inputs to have zero mean and unit variance. Weight normalization reparameterizes the weight vectors in a neural network that decouples the length of those weight vectors from their direction [21], inspired by batch normalization. In other words, by their L2-norm or L1-norm [22], weight normalization reparameterizes incoming weights.

The L1-norm uses the sum of all the values providing equal penalty to all parameters, enforcing sparsity:

$$X'_i = \frac{X_i}{\sum_{k=0}^n X_k} \quad (6)$$

Similarly, the L2-norm uses the square root of the sum of all the squared values.

$$X'_i = \frac{X_i}{\sum_{k=0}^n X_k^2} \quad (7)$$

In all cases, X_i is the value to be normalized, and X'_i is the normalized score.

The post-processing normalization method consists of the independent normalization of each derived descriptor (L1-norm and L2-norm Axis-1), the normalization of each characteristic (L1-norm and L2-norm Axis-0), and the scaling of *ROBUST*.

$$X'_i = \frac{X_i - q_1(X_i)}{q_2(X_i) - q_1(X_i)} \quad (8)$$

where q_1 and q_2 are quantiles.

The scaling normalization of *ROBUST* eliminates the median. It scales the data according to the quantile range, meaning that the sample mean and variance are not affected by the outliers.

A. Retrieval Results

Tables I, II, III and IV list the image retrieval performance on the INRIA, UKBench, Paris6K and Oxford5K datasets respectively. The first conclusion that emerges by observing the results is that the ViT descriptor performs remarkably well with almost all the different similarity metrics and all the normalization techniques in all four image datasets. In all experiments, the Chebyshev metric significantly lags behind the effectiveness of the other distance metrics.

TABLE I
EXPERIMENTAL RESULTS ON INRIA DATABASE

Model	INRIA						
	Manh.	Eucl.	Cos	BC	Canb.	Cheb.	Correl.
ViT-L16							
L2 Axis=1	84.95	84.98	84.98	84.88	84.62	76.24	84.97
L2 Axis=0	85.02	85.24	85.36	85.07	84.54	77.67	85.36
L1 Axis=1	84.77	84.88	84.98	84.91	84.67	76.26	84.97
L1 Axis=0	85.02	85.23	85.53	85.08	84.54	78.02	85.52
ROBUST	84.98	85.10	86.31	86.08	85.50	76.71	86.31
ViT-L32							
L2 Axis=1	86.84	86.56	86.56	86.77	86.32	75.90	86.56
L2 Axis=0	86.65	86.61	86.96	86.92	86.30	76.34	86.96
L1 Axis=1	86.88	86.57	86.56	86.78	86.32	75.45	86.56
L1 Axis=0	86.65	86.64	86.97	86.92	86.30	76.52	86.97
ROBUST	86.61	86.61	87.03	87.05	86.80	76.83	87.03
ViT-B16							
L2 Axis=1	87.16	87.09	87.09	87.17	86.57	75.77	87.09
L2 Axis=0	86.79	86.53	86.76	87.26	86.55	77.95	87.67
L1 Axis=1	87.18	86.97	87.09	87.18	86.58	75.30	87.09
L1 Axis=0	86.78	86.51	87.67	87.29	86.55	77.31	87.67
ROBUST	86.42	86.33	87.99	87.81	87.32	77.07	87.99
ViT-B32							
L2 Axis=1	85.07	84.80	84.80	85.19	84.61	62.52	84.80
L2 Axis=0	84.97	85.04	85.61	85.38	84.74	77.96	85.61
L1 Axis=1	85.31	84.96	84.80	85.19	84.76	61.84	84.80
L1 Axis=0	84.98	84.93	85.63	85.38	84.74	77.25	85.63
ROBUST	84.96	85.07	86.11	86.22	85.32	76.85	86.11

TABLE II
EXPERIMENTAL RESULTS ON UKBENCH DATABASE

Model	UKBench						
	Manh.	Eucl.	Cos	BC	Canb.	Cheb.	Correl.
ViT-L16							
L2 Axis=1	3.782	3.785	3.785	3.781	3.764	3.561	3.785
L2 Axis=0	3.778	3.78	3.785	3.782	3.764	3.575	3.785
L1 Axis=1	3.781	3.783	3.785	3.781	3.764	3.56	3.785
L1 Axis=0	3.778	3.781	3.785	3.782	3.764	3.574	3.785
ROBUST	3.777	3.779	3.784	3.781	3.763	3.567	3.784
ViT-L32							
L2 Axis=1	3.75	3.752	3.752	3.75	3.73	3.416	3.752
L2 Axis=0	3.735	3.737	3.754	3.751	3.731	3.455	3.754
L1 Axis=1	3.752	3.751	3.752	3.75	3.731	3.412	3.752
L1 Axis=0	3.735	3.737	3.754	3.751	3.731	3.453	3.754
ROBUST	3.735	3.737	3.749	3.747	3.729	3.455	3.749
ViT-B16							
L2 Axis=1	3.745	3.746	3.746	3.745	3.728	3.345	3.746
L2 Axis=0	3.733	3.737	3.758	3.752	3.729	3.496	3.758
L1 Axis=1	3.746	3.746	3.746	3.746	3.729	3.34	3.746
L1 Axis=0	3.733	3.737	3.758	3.752	3.729	3.496	3.758
ROBUST	3.733	3.737	3.759	3.752	3.733	3.496	3.759
ViT-B32							
L2 Axis=1	3.712	3.702	3.702	3.712	3.692	2.971	3.702
L2 Axis=0	3.709	3.714	3.725	3.718	3.693	3.442	3.725
L1 Axis=1	3.711	3.701	3.702	3.712	3.693	2.952	3.702
L1 Axis=0	3.709	3.714	3.725	3.717	3.693	3.439	3.725
ROBUST	3.709	3.714	3.726	3.722	3.697	3.45	3.726

A more in-depth analysis of the results also reveals that the ViT-B16 descriptor performs robustly well in all databases. Of course, in the UKBench dataset, the ViT-L16 descriptor manages to exceed the performance of the ViT-B16 descriptor slightly, but the difference is not significant to generalize a conclusion. The ViT-B16 descriptor presents high retrieval accuracy, promoting robustness in all datasets and almost all the different similarity metrics.

Regarding the normalization techniques, *ROBUST* scaling appears to be the optimal solution. Moreover, one quickly concludes that the *ROBUST* normalization technique, together with the Cosine distance as the similarity metric, shape the descriptor’s most effective setup. This combination manages to outperform any other design in all performed experiments. Thus, it is safe to conclude that the combination of the ViT-B16 model, with *ROBUST* normalization and Cosine distance as similarity metric, shapes a robust plug-and-play solution for effective image retrieval.

TABLE III
EXPERIMENTAL RESULTS ON PARIS6K DATABASE

Model	Paris6k						
	Manh.	Eucl.	Cos	BC	Canb.	Cheb.	Correl.
ViT-L16							
L2 Axis=1	86.24	86.23	86.23	86.25	85.82	77.34	86.25
L2 Axis=0	86.27	86.24	86.63	86.46	85.82	76.16	86.63
L1 Axis=1	86.17	86.15	86.23	86.25	85.82	77.17	86.25
L1 Axis=0	86.25	86.23	86.64	86.47	85.82	75.97	86.64
ROBUST	86.18	86.13	86.74	86.71	86.38	76.16	86.74
ViT-L32							
L2 Axis=1	85.29	85.34	85.34	85.41	85.09	72.56	85.34
L2 Axis=0	84.48	84.47	85.68	85.65	85.11	69.76	85.68
L1 Axis=1	85.37	85.42	85.34	85.41	85.1	72.6	85.34
L1 Axis=0	84.45	84.45	85.69	85.65	85.11	69.57	85.69
ROBUST	84.4	84.35	85.62	85.61	85.18	69.04	85.62
ViT-B16							
L2 Axis=1	86.94	87.07	87.07	86.85	86.25	75.96	87.07
L2 Axis=0	86.28	86.23	87.21	86.97	86.27	77.26	87.21
L1 Axis=1	86.93	87.06	87.07	86.84	86.25	75.72	87.07
L1 Axis=0	86.27	86.2	87.23	86.99	86.27	77.06	87.23
ROBUST	86.43	86.46	87.83	87.63	87.06	76.61	87.83
ViT-B32							
L2 Axis=1	85.53	85.29	85.29	85.56	85.24	64.04	85.28
L2 Axis=0	85.34	85.29	85.95	85.83	85.23	75.96	85.94
L1 Axis=1	85.5	85.19	85.29	85.56	85.23	63.55	85.28
L1 Axis=0	85.34	85.27	85.96	85.83	85.23	75.77	85.96
ROBUST	85.29	85.24	86.32	86.35	85.9	75.51	86.32

TABLE IV
EXPERIMENTAL RESULTS ON OXFORD5K DATABASE

Model	Oxford5k						
	Manh.	Eucl.	Cos	BC	Canb.	Cheb.	Correl.
ViT-L16							
L2 Axis=1	60.84	60.82	60.82	60.78	59.87	51.49	60.83
L2 Axis=0	60.9	61.20	61.50	61.15	59.85	53.26	61.50
L1 Axis=1	60.73	60.74	60.82	60.78	59.85	51.21	60.83
L1 Axis=0	60.91	61.13	61.58	61.2	59.85	53.12	61.58
ROBUST	60.82	60.86	62.37	62.09	61.49	52.45	62.37
ViT-L32							
L2 Axis=1	55.17	55.3	55.30	55.01	53.84	41.26	55.28
L2 Axis=0	54.92	55.14	55.55	55.21	53.84	41.45	55.55
L1 Axis=1	55.35	55.43	55.3	55.01	53.86	41.39	55.28
L1 Axis=0	54.93	55.18	55.56	55.23	53.84	41.31	55.56
ROBUST	54.93	55.19	56.30	55.88	55.16	41.78	56.30
ViT-B16							
L2 Axis=1	63.24	63.59	63.59	63.22	62.17	52.44	63.59
L2 Axis=0	62.74	63.16	64.19	63.53	62.12	56.79	64.19
L1 Axis=1	63.13	63.68	63.59	63.26	62.13	52.3	63.59
L1 Axis=0	62.79	63.14	64.22	63.55	62.12	56.48	64.22
ROBUST	62.72	63.05	64.68	64.09	62.84	56.02	64.68
ViT-B32							
L2 Axis=1	63.18	62.49	62.49	63.08	62.84	41.78	62.49
L2 Axis=0	63.34	63.01	63.56	63.52	62.82	53.96	63.56
L1 Axis=1	63.19	62.41	62.49	63.1	62.8	41.33	62.49
L1 Axis=0	63.35	62.99	63.59	63.54	62.82	53.78	63.59
ROBUST	63.35	63.09	64.43	64.28	63.35	53.99	64.43

B. Comparison with the State-of-the-art

This subsection compares the ViT descriptor’s performance with the state-of-the-art local, global, and deep convolutional-based approaches from the recent literature. The proposed descriptor was compared to 36 descriptors from the literature. The choice of the descriptors used for experimentation was primarily based on their reported performance and overall popularity. The descriptors are listed in Table V and sorted based on their retrieval performance on the INRIA dataset. The reason for choosing this sorting method is related to the fact that most of the descriptors/approaches reported in this subsection have been evaluated on the INRIA dataset and their retrieval results are publicly available or reproducible.

Experimental findings show that the ViT descriptor performs robustly and provides remarkable results in all benchmarking datasets. The results in Table V demonstrate that the presented approach performs as good as the state-of-the-art approaches on all datasets. Moreover, the acquired retrieval results are among the leading published ones and are directly comparable with the literature’s best reported.

TABLE V

RETRIEVAL SCORE PER IMAGE COLLECTION. THIS PAPER USES MAP (MEAN AVERAGE PRECISION) TO EVALUATE RETRIEVAL ACCURACY ON THE INRIA (HOLIDAYS), PARIS6K, AND OXFORD5K DATASETS. THE N-S SCORE IS SPECIFICALLY USED ON THE UKBENCH DATASET. (†) REFERS TO RESULTS THAT ARE REPORTED IN [23], [24]

Retrieval Method	INRIA	UKBen.	Paris	Oxford
MMF-HC [25]	94.1	3.87	-	-
MR Spatial search [26]	89.6	-	87.9	84.3
GatedSQU [23]	88.8	3.74	81.3	69.4
ViT-16B	88.0	3.76	87.8	64.7
ASMK+SA (large) [27]	88.0	-	78.7	82.0
ASMK+MA (large) [27]	86.5	-	80.5	83.8
Zheng Et al. (PPS) [28]	85.2	3.79	-	-
R-mac [29]	85.2(†)	3.74(†)	83.0	66.9
R-mac-RPN [24]	86.7	-	87.1	83.1
CroW [30]	85.1	3.63(†)	79.7	70.8
MMF-SIFT [25]	84.4	3.94	-	-
CNNaug-ss [31]	84.3	-	46.0	36.0
SMK+SA (large) [27]	84.0	-	73.2	78.5
HE+WGC [32]	81.3	3.42	61.5	51.6
GoogleNet [31]	83.6	-	58.3	55.8
ReDSL.FC1 [33]	-	-	94.7	78.3
R101-DELG [34]	-	-	82.9	78.5
Varga et al. [35]	-	-	-	74.4
SMK+MA (large) [27]	82.9	-	74.2	79.3
CVLad [36]	82.7	3.62	-	51.4
OxfordNet [31]	81.6	-	59.0	59.3
Local CoMo [37]	81.1	-	-	-
CNN+BoVW [38]	80.2	-	-	-
MOP-CNN [39]	80.2	-	-	-
Patch-CKN [40]	79.3	3.76	-	56.5
Neural codes [41]	79.3	3.29	-	54.5
Alexet-conv3 [42]	79.3	3.76	-	43.4
LBOW [15]	78.9	3.50	-	-
Alexet-conv4 [42]	77.1	3.73	-	34.3
SaCoCo [43]	76.1	3.33	-	-
Alexet-conv5 [42]	75.3	3.69	-	47.7
PhilippNet [44]	74.1	3.66	-	-
CEDD [45]	72.6	3.06	-	-
CoMo [37]	72.6	-	-	-
Alexet-conv2 [42]	62.7	3.19	-	12.5
Alexet-conv1 [42]	59.0	3.33	-	18.8
BoVW [15]	57.2	2.95	-	-

In the INRIA and UKBench datasets, the shaped solution presents the fourth-best reported result. In the case of the Paris6K dataset, the ViT descriptor reports the third-best performance. Finally, in the Oxford5K dataset, the ViT descriptor’s effectiveness is comparable with the CNN-based image retrieval approaches. It is noteworthy that the full image is used as a query in both Oxford5K and Paris6K datasets instead of the annotated region of interest.

In a nutshell, the ViT descriptor significantly outperforms all the handcrafted features and most machine-crafted, CNN-based ones in all the datasets. Of course, the literature contains more sophisticated methods and algorithms that exceed the shaped descriptor’s retrieval accuracy. But once again, it is worth noting that the ViT descriptor is ready to use, plug-and-play descriptor, and no training or parameter fitting is needed. The vast majority of the listed deep-learning-based approaches are considerably more complicated and demanding than the ViT solution.

For example, in [25], a multi-index fusion scheme for image retrieval was proposed based on AlexNet and ResNet50 networks. The method is called MMF and inherits the core idea of Collaborative Index Embedding to fuse different visual representations on an index level. Furthermore, MMF explores the high-order information assumed by considering the sparse index structure for retrieval, an inverted index structure's intrinsic property. The impressive performance reported by [25] requires the creation and learning of an index-specific functional matrix to propagate similarities and the application of an Augmented Lagrange Multiplier (ALM) to optimize multi-index fusion. By taking into account various factors such as geometric invariance, layers, and search efficiency, an optimized CNN architecture was created and trained. This architecture is known as MR Spatial search [26]. It is important to note that the MR Spatial search performs a costly spatial verification at test-time. The authors in [23] focuses on global feature pooling over CNN activations for image instance retrieval. The descriptor is called GatedSQU, and it contains the design of a channel-wise pooling and learning with triplet Loss. The authors in [35] combined a semantic-level similarity and a feature-level similarity to efficiently calculate the similarity distance. The authors perform a comprehensive series of analytical studies in [33], aimed at forming more efficient representations of features. Finally, it is worth noting that ReDSL.FC1 method significantly outperforms all reported methods on Paris and Oxford datasets as the authors fine-tuned the pre-trained CNN architecture directly on these landmarks using similarity learning.

The experiments were conducted on a workstation with AMD Ryzen 7 1700, 32GB RAM, and GTX 1080 GPU using the *KERAS* framework [46], a well-known high-level Python neural network library that runs on top of TensorFlow or Theano. Vision Transformer's implementation is based on the open-source release of the network available on GitHub¹.

IV. CONCLUSIONS

This paper presents a fully unsupervised, parameter-free image retrieval descriptor. Overall, the shaped solution appears to be suitable for content-based image retrieval tasks. The experimental evaluation findings on several different datasets clearly shown that the proposed approach managed to outperform many state-of-the-art, more sophisticated, and complex solutions from the literature. Although the ViT descriptor does not supersede all the other methods, it is safe to conclude that it brings a new approach to the image retrieval domain. A critical direction to improve image retrieval performance is to revisit the well-established CNN-based methods in the literature and replace the backbone pre-trained network with the vision transformers. A new chapter in the image retrieval scientific subject is looming.

¹<https://github.com/faustomorales/vit-keras>

- [1] L. Zheng, Y. Yang, and Q. Tian, "Sift meets cnn: A decade survey of instance retrieval," *IEEE transactions on pattern analysis and machine intelligence*, vol. 40, no. 5, pp. 1224–1244, 2018.
- [2] A. Vaswani, N. Shazeer, N. Parmar, J. Uszkoreit, L. Jones, A. N. Gomez, Ł. Kaiser, and I. Polosukhin, "Attention is all you need," *Advances in neural information processing systems*, vol. 30, pp. 5998–6008, 2017.
- [3] X. Wang, R. Girshick, A. Gupta, and K. He, "Non-local neural networks," in *Proceedings of the IEEE conference on computer vision and pattern recognition*, 2018, pp. 7794–7803.
- [4] K. Han, Y. Wang, H. Chen, X. Chen, J. Guo, Z. Liu, Y. Tang, A. Xiao, C. Xu, Y. Xu *et al.*, "A survey on visual transformer," *arXiv preprint arXiv:2012.12556*, 2020.
- [5] F. Locatello, D. Weissenborn, T. Unterthiner, A. Mahendran, G. Heigold, J. Uszkoreit, A. Dosovitskiy, and T. Kipf, "Object-centric learning with slot attention," *arXiv preprint arXiv:2006.15055*, 2020.
- [6] H. Hu, J. Gu, Z. Zhang, J. Dai, and Y. Wei, "Relation networks for object detection," in *Proceedings of the IEEE Conference on Computer Vision and Pattern Recognition*, 2018, pp. 3588–3597.
- [7] M. Chen, A. Radford, R. Child, J. Wu, H. Jun, D. Luan, and I. Sutskever, "Generative pretraining from pixels," in *International Conference on Machine Learning*. PMLR, 2020, pp. 1691–1703.
- [8] A. Dosovitskiy, L. Beyer, A. Kolesnikov, D. Weissenborn, X. Zhai, T. Unterthiner, M. Dehghani, M. Minderer, G. Heigold, S. Gelly *et al.*, "An image is worth 16x16 words: Transformers for image recognition at scale," *arXiv preprint arXiv:2010.11929*, 2020.
- [9] J. Devlin, M.-W. Chang, K. Lee, and K. Toutanova, "Bert: Pre-training of deep bidirectional transformers for language understanding," *arXiv preprint arXiv:1810.04805*, 2018.
- [10] T. B. Brown, B. Mann, N. Ryder, M. Subbiah, J. Kaplan, P. Dhariwal, A. Neelakantan, P. Shyam, G. Sastry, A. Askell, S. Agarwal, A. Herbert-Voss, G. Krueger, T. Henighan, R. Child, A. Ramesh, D. M. Ziegler, J. Wu, C. Winter, C. Hesse, M. Chen, E. Sigler, M. Litwin, S. Gray, B. Chess, J. Clark, C. Berner, S. McCandlish, A. Radford, I. Sutskever, and D. Amodei, "Language models are few-shot learners," 2020.
- [11] Q. Wang, B. Li, T. Xiao, J. Zhu, C. Li, D. Wong, and L. Chao, "Learning deep transformer models for machine translation," 01 2019, pp. 1810–1822.
- [12] J. L. Ba, J. R. Kiros, and G. E. Hinton, "Layer normalization," *arXiv preprint arXiv:1607.06450*, 2016.
- [13] J. Deng, W. Dong, R. Socher, L. Li, Kai Li, and Li Fei-Fei, "Imagenet: A large-scale hierarchical image database," in *2009 IEEE Conference on Computer Vision and Pattern Recognition*, 2009, pp. 248–255.
- [14] H. Jegou, M. Douze, and C. Schmid, "Hamming embedding and weak geometric consistency for large scale image search," in *Computer Vision – ECCV 2008*, D. Forsyth, P. Torr, and A. Zisserman, Eds. Berlin, Heidelberg: Springer Berlin Heidelberg, 2008, pp. 304–317.
- [15] C. Wengert, M. Douze, and H. Jégou, "Bag-of-colors for improved image search," in *Proceedings of the 19th ACM International Conference on Multimedia*, ser. MM '11. New York, NY, USA: ACM, 2011, pp. 1437–1440. [Online]. Available: <http://doi.acm.org/10.1145/2072298.2072034>
- [16] J. Philbin, O. Chum, M. Isard, J. Sivic, and A. Zisserman, "Lost in quantization: Improving particular object retrieval in large scale image databases," in *Computer Vision and Pattern Recognition, 2008. CVPR 2008. IEEE Conference on*. IEEE, 2008, pp. 1–8.
- [17] —, "Object retrieval with large vocabularies and fast spatial matching," in *2007 IEEE conference on computer vision and pattern recognition*. IEEE, 2007, pp. 1–8.
- [18] V. R. Chandrasekhar, D. M. Chen, S. S. Tsai, N.-M. Cheung, H. Chen, G. Takacs, Y. Reznik, R. Vedantham, R. Grzeszczuk, J. Bach *et al.*, "The stanford mobile visual search data set," in *Proceedings of the second annual ACM conference on Multimedia systems*, 2011, pp. 117–122.
- [19] S. Chatzichristofis, C. Iakovidou, Y. Boutalis, and E. Angelopoulou, "Mean normalized retrieval order (mnro): a new content-based image retrieval performance measure," *Multimedia Tools and Applications*, pp. 1–32, 2012. [Online]. Available: <http://dx.doi.org/10.1007/s11042-012-1192-z>
- [20] S. Patil and S. Talbar, "Content based image retrieval using various distance metrics," in *Data Engineering and Management*, R. Kannan and F. Andres, Eds. Berlin, Heidelberg: Springer Berlin Heidelberg, 2012, pp. 154–161.

- [21] T. Salimans and D. P. Kingma, "Weight normalization: A simple reparameterization to accelerate training of deep neural networks," in *Advances in neural information processing systems*, 2016, pp. 901–909.
- [22] S. Wu, G. Li, L. Deng, L. Liu, D. Wu, Y. Xie, and L. Shi, "l1-norm batch normalization for efficient training of deep neural networks," *IEEE transactions on neural networks and learning systems*, vol. 30, no. 7, pp. 2043–2051, 2018.
- [23] Z. Chen, J. Lin, V. Chandrasekhar, and L.-Y. Duan, "Gated square-root pooling for image instance retrieval," in *2018 25th IEEE International Conference on Image Processing (ICIP)*. IEEE, 2018, pp. 1982–1986.
- [24] A. Gordo, J. Almazán, J. Revaud, and D. Larlus, "Deep image retrieval: Learning global representations for image search," in *European conference on computer vision*. Springer, 2016, pp. 241–257.
- [25] Z. Zhang, Y. Xie, W. Zhang, and Q. Tian, "Effective image retrieval via multilinear multi-index fusion," *IEEE Transactions on Multimedia*, 2019.
- [26] A. S. Razavian, J. Sullivan, S. Carlsson, and A. Maki, "Visual instance retrieval with deep convolutional networks," *ITE Transactions on Media Technology and Applications*, vol. 4, no. 3, pp. 251–258, 2016.
- [27] G. Toliás, Y. S. Avrithis, and H. Jégou, "Image search with selective match kernels: Aggregation across single and multiple images," *International Journal of Computer Vision*, vol. 116, no. 3, pp. 247–261, 2016.
- [28] L. Zheng, S. Wang, and Q. Tian, "Coupled binary embedding for large-scale image retrieval," *Image Processing, IEEE Transactions on*, vol. 23, no. 8, pp. 3368–3380, 2014.
- [29] G. Toliás, R. Sicre, and H. Jégou, "Particular object retrieval with integral max-pooling of cnn activations," *arXiv preprint arXiv:1511.05879*, 2015.
- [30] Y. Kalantidis, C. Mellina, and S. Osindero, "Cross-dimensional weighting for aggregated deep convolutional features," in *European conference on computer vision*. Springer, 2016, pp. 685–701.
- [31] J. Yue-Hei Ng, F. Yang, and L. S. Davis, "Exploiting local features from deep networks for image retrieval," in *Proceedings of the IEEE conference on computer vision and pattern recognition workshops*, 2015, pp. 53–61.
- [32] H. Jégou, M. Douze, and C. Schmid, "Improving bag-of-features for large scale image search," vol. 87, no. 3, 2010, pp. 316–336. [Online]. Available: <https://doi.org/10.1007/s11263-009-0285-2>
- [33] J. Wan, D. Wang, S. C. H. Hoi, P. Wu, J. Zhu, Y. Zhang, and J. Li, "Deep learning for content-based image retrieval: A comprehensive study," in *Proceedings of the 22nd ACM international conference on Multimedia*, 2014, pp. 157–166.
- [34] B. Cao, A. Araujo, and J. Sim, "Unifying deep local and global features for image search," in *European Conference on Computer Vision*. Springer, 2020, pp. 726–743.
- [35] D. Varga and T. Szirányi, "Fast content-based image retrieval using convolutional neural network and hash function," in *2016 IEEE international conference on systems, man, and cybernetics (SMC)*. IEEE, 2016, pp. 002 636–002 640.
- [36] W.-L. Zhao, H. Jégou, and G. Gravier, "Oriented pooling for dense and non-dense rotation-invariant features," 2013.
- [37] S. A. Vassou, N. Anagnostopoulos, K. Christodoulou, A. Amanatiadis, and S. A. Chatzichristofis, "Como: a scale and rotation invariant compact composite moment-based descriptor for image retrieval," *Multimedia Tools and Applications*, pp. 1–24, 2018.
- [38] A. Sharif Razavian, H. Azizpour, J. Sullivan, and S. Carlsson, "Cnn features off-the-shelf: an astounding baseline for recognition," in *Proceedings of the IEEE conference on computer vision and pattern recognition workshops*, 2014, pp. 806–813.
- [39] Y. Gong, L. Wang, R. Guo, and S. Lazebnik, "Multi-scale orderless pooling of deep convolutional activation features," in *Computer Vision - ECCV 2014 - 13th European Conference, Zurich, Switzerland, September 6-12, 2014, Proceedings, Part VII*, 2014, pp. 392–407.
- [40] M. Paulin, M. Douze, Z. Harchaoui, J. Mairal, F. Perronnin, and C. Schmid, "Local convolutional features with unsupervised training for image retrieval," in *2015 IEEE International Conference on Computer Vision, ICCV 2015, Santiago, Chile, December 7-13, 2015*, 2015, pp. 91–99.
- [41] A. Babenko, A. Slesarev, A. Chigorin, and V. Lempitsky, "Neural codes for image retrieval," in *European conference on computer vision*. Springer, 2014, pp. 584–599.
- [42] M. Paulin, M. Douze, Z. Harchaoui, J. Mairal, F. Perronnin, and C. Schmid, "Local convolutional features with unsupervised training for image retrieval," in *Proceedings of the IEEE international conference on computer vision*, 2015, pp. 91–99.
- [43] C. Iakovidou, N. Anagnostopoulos, M. Lux, K. Christodoulou, Y. S. Boutalis, and S. A. Chatzichristofis, "Composite description based on salient contours and color information for CBIR tasks," *IEEE Trans. Image Processing*, vol. 28, no. 6, pp. 3115–3129, 2019. [Online]. Available: <https://doi.org/10.1109/TIP.2019.2894281>
- [44] P. Fischer, A. Dosovitskiy, and T. Brox, "Descriptor matching with convolutional neural networks: a comparison to sift," *arXiv preprint arXiv:1405.5769*, 2014.
- [45] S. A. Chatzichristofis and Y. S. Boutalis, "Cedd: Color and edge directivity descriptor: A compact descriptor for image indexing and retrieval," in *ICVS*, 2008, pp. 312–322.
- [46] A. Gulli and S. Pal, *Deep learning with Keras*. Packt Publishing Ltd, 2017.